Cluster analysis and petrophysical relationships for a geothermal reservoir in La Garriga area

Author: María Blanch Jover
Facultat de Física, Universitat de Barcelona, Diagonal 645, 08028 Barcelona, Spain.

Advisor: Pilar Neus Queralt Capdevila

Abstract: Porosity is a key parameter to appraise the geothermal potential of a reservoir. However, its determination is complex because it is not possible measure it direct, except when taking samples. The use of empirical laws to link porosity with geophysical properties can be an indirect way to determine it for different geological units present in an area of interest. Clustering methods have been used to jointly interpret seismic tomography and resistivity models from Valles Fault, near La Garriga, a geothermal area of interest. For each cluster, empirical laws that relate geophysical properties with porosity have been adjusted with porosity values that were obtained previously in the laboratory.

I. INTRODUCTION

The recent increase in energy consumption, the limited amount of fossil fuels and the negative impact that these have on the environment has lead to an increase on the research for cleaner sources of energy [1]. Among these, geothermal energy plays a very important role due to its continuous generation of energy and its relatively cheap extraction.

Geothermal systems can be classified depending on the temperature of its fluids. High-temperature geothermal systems have larger capacity and, due to the high gradient contrast, are easy to characterize with geophysical methods. Among them, electrical and seismic are the most common methods. However, in medium and low-temperature systems, sometimes there is an insufficient physical contrast form the host rock to easily detect the geothermal reservoir [2]. In addition to geophysical properties that characterise the geometry and physical properties of the reservoir rocks, it is necessary to determine petrophysical properties, such as porosity. To determine the geothermal potential of the reservoir, the porosity is needed.

In La Garriga area there are several hot springs where water comes out at around 60°C [2]. This makes it an area of geothermal interest due to its possible potential to generate energy in a renewable way.

For a geothermal study it is necessary to calculate the capacity of the reservoir. With this purpose, porosity and permeability are estimated. Porosity can be acquire by collecting rock samples and doing measurements in the laboratory. It can also be determinate indirectly with the empirical laws that relate porosity with seismic velocity or resistivity. However, a joint interpretation of seismic and resistivity models allows a better characterization of the rocks. To calibrate these empirical relationships, both geophysical and petrophysical data are needed.

The purpose of this study is to find the empirical laws that relate porosity with geophysical properties for the study area. For a better characterization, geophysical properties have been combined.

II. TOMOGRAPHY MODELS

In the frame of a current researcher project of the Geophysics department of the University of Barcelona, a seismic and an electrical tomography were obtained. Figure 1 shows the location where tomographies were taken, next to La Garriga Village, in the Vallès-Penedès fault area. This separates the Costal and Pre-Costal ranges by a horst and graben system [3].

The purpose of the study was the characterization of the most superficial materials of the area adjacent to the fault. For this study, it has been possible to use the inverted models of these tomographies.

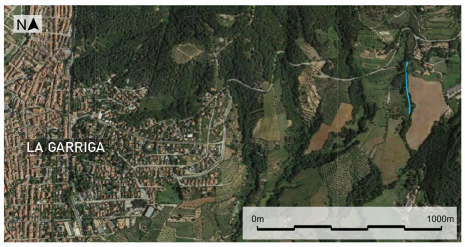

FIG. 1: Relative position of the location where tomographies values where taken respect La Garriga village.

All the data processing and the obtaining of images and graphs have been done using MATLAB.

A. Electrical resistivity tomography

Figure 2 shows the representation of the inverted model of the 2D Electrical Resistivity Tomography (ERT). The color scale is in logarithmic scale.

The resistivity varies from 3 up to 200 Ω·m. The ERT show different areas based on the different resistivity values:

- From x=0 to x=150m the subsoil is characterized for having the highest resistivities. They vary from

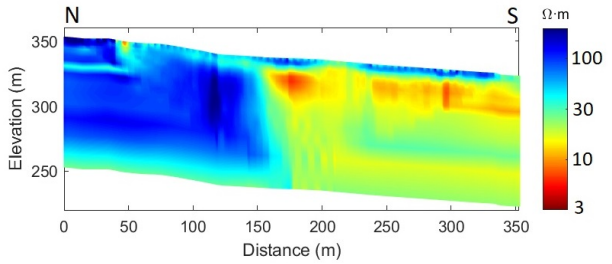

FIG. 2: 2D ERT inversion model.

40 Ω·m up to the highest resistivity in the profile.

- From x=150 to x=350m low resistivities can be seen in the lower parts of the profile. They vary up to 16 Ω·m. Some low resistivity zones can also be seen in this section with values from 3 to 7 Ω·m.
- The last section would be the upper part where there is a high resistivity zone for all the length of the profile. The value range is similar to the first section, from 40 Ω·m to 200 Ω·m, with a small zone around x=47m where it drops to 10 Ω·m.

The ERT profile shows a clear division of the underground, separating a low resistivity zone in the south of the profile with a high one in the north. It can easily be interpreted that is in this division where the Vellès-Penedès fault is located.

B. Seismic tomography

Figure 3 show the representation of the P waves seismic model. The seismic model shows a clear increase in

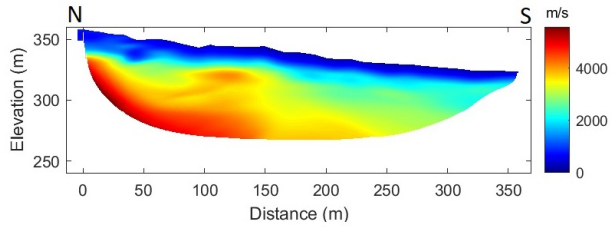

FIG. 3: P waves seismic model.

velocity with depth. However, it can also be divided in three:

- The superficial part of the profile is characterized by low velocities. These vary from 270m/s to 2500m/s.
- In the northern part of the profile there is a high velocity section. The range of values is from 2500m/s to 5500m/s.
- The southern part of the profile has medium velocity values that are quite constant through the section. These varies from 2500m/s to 3500m/s.

III. CLUSTERING

Adjusting the equations for the whole area is complicated due to the great variation of velocity and resistivity values in the profile. Therefore, it has been divided into subzones combing the range of the resistivies and velocities of our models.
One method to do this is Fuzzy Cluster Method or fuzzy c-means clustering which classifies the data into n fuzzy clusters [4]. Each data point partially belongs to a certain degree to every cluster by having a membership value for each of them. This value is based on the Euclidian distance of the data point to the center of the cluster. Each data point is assigned to the cluster with the highest membership value.
The two tomographies were coincident, but they did not have the same length or dimension. The 2D ERT inverted model had a 215x19 data matrix while the seismic tomography model had a 611x212 data matrix. Since the given data had to be in a two-dimension vector, $(x_i(\rho_i, v_i))$, some changes were made.
First, it was searched which area of the profile had both velocity and resistivity values. The seismic tomography was also downshaped to the resistivity matrix in order to have the same number of points. An attempt to obtain the clusters with these points was made but the program only took into account for the division of the zones the variation of the velocity. Therefore, the resistivity was put in logarithmic scale and the given values were normalized.
The clustering method only considers the given values and does not take into account the position of the data points in the profile. That is why the group to which some points belonged was changed by hand. However, it was taken care that the values of resistivity and seismic velocity did not deviate to much from the ones of their new cluster.

A. Clustering results

A 350m length fuzzy c-means images with a elevation that goes from 350 to 240m and a 215x19 data grid was obtained. The number of clusters had to be selected by hand. It was tested with different numbers to see the main differences of the clusters disposition. In figure A.4 can be seen the profile for different numbers of clusters and in figure A.5 the value range for each cluster of resisitivity and seismic velocity can be seen. Finally, a number of five clusters was chosen.

Looking at figure 4, there are three main units, which correspond to the mentioned above: A, B and C. These last two have been divided in two subunits.
Cluster A, in the northern part of the profile, has a high resistivity and velocity values. It would correspond to fracturated granodiorite. It has a higher resistivity than

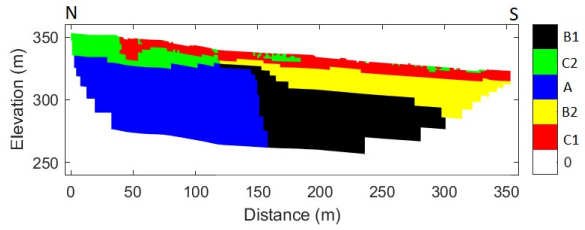

FIG. 4: Representation of the clusters.

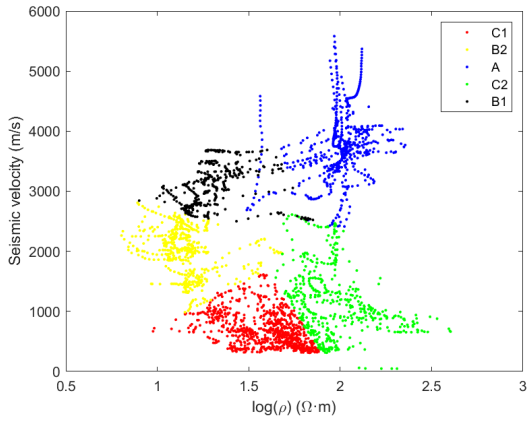

FIG. 5: Seismic velocity vs resistivity. Each point has been colored according to the cluster to which it belongs.

expected for a basement [5]. This could be due to its fracturing and to hydrothermal alteration.
Cluster B, in the southern part of the profile, has mid-velocity values and low resistivity values. It would correspond to a silt and clay deposits of the Miocene [5]. In the ERT some small zones with lower resistivities can be found in this unit. These are contained in B2 and can be interpreted as fine-grained (clay) deposits, while B1 would be sandstones and silts.
Cluster C, in the upper part of the profile, has low velocity values and a wide range of resistivity values. C2 would be altered granodiorite whereas C1 is a result of the Quaternary processes [5].

IV. RESULTS

Porosity is a dimensionless intrinsic property of the materials that gives the percentage of empty space of the material. Porosity can be acquire by collecting sample of the land and doing measurements in the laboratory. It can also be determinate indirectly with empirical laws that relate porosity with for example seismic velocity or resistivity.
Clusters B1, B2 and C1, which correspond to unconsolidated rocks, are sediments. For these formations the porosity is primary, which is the space that exist between the grains where fluids or thin layers of clay can be hold.
Clusters A and C2 are crystalline or hard material. They can be fractured due to hydrothermal alteration. Fractures can be considered a secondary porosity where fluid or clay can be hold.

A. Petrophysical relationships

Many authors have found empirical laws that relate porosity to other physical properties [6]. However, these laws vary depending on the material on the specific site, that is why it is necessary to adjust them each time.
The p-waves seismic velocity and porosity equation for consolidated rocks [6] can be written as:

$$v_p = (1-\phi)^2 \cdot v_{matrix} + \phi \cdot v_{pore}, \tag{1}$$

where v_{matrix} is the seismic velocity of the rock grains and v_{pore} of the pore fluid. However, this equation can not be easily used and it does not take into account clay content, which experiments show that it decreases the velocity [6]. That is why many authors use an empirical relationship that has the form:

$$v_p = H_0 - H_1 \cdot \phi - H_2 \cdot C, \tag{2}$$

where C is volumetric clay content and H_0, H_1 and H_2 are constants with velocity units that need to be adjusted. This equation has a linear dependence on porosity and clay content and porosity cause a decrease in velocity.
Another empirical law would be Archies', which gives the relationship between resistivity and porosity. However, a slightly modified version of this law has the form [6]:

$$\rho = \rho_w \cdot a \cdot \phi^{-m} \cdot S_w^{-n}, \tag{3}$$

where ρ_w is the resistivity of the water saturated pore, a is an dimensionless proportional constant, S_w is the fraction of pore space filled with water, n is the saturation exponent, ϕ is the porosity and m is the cementation exponent. The original Archies law did not consider the fraction of pore space filled with water term.
For clayey materials the calculation of resistivity is complicated because it can also conduct electric current. Frohlich and Parke found the following relationship [6]:

$$\frac{1}{\rho} = \frac{\phi^m \cdot S_w^n}{a \cdot \rho_w} + \frac{1}{\rho_s}, \tag{4}$$

where the term ρ_s is the surface resistivity and it can be calculated with the following expression found by Rhoades [6]:

$$\frac{1}{\rho_s} = D1 \cdot C - D2, \tag{5}$$

where C is the volumetric clay content and D1 and D2 are constants with units of resistivity that need to be adjusted.

B. Porosity values

Due to the geothermal interest in this area many studies are being carried out. In one of them, some subsoil samples were obtained and their porosity was studied in a laboratory. It was possible to have access to these porosity data obtained by Mitjanas(2021) [7] in the Technical University Bergakademie Freiberg, in Germany. The position of where the sample was obtained can be seen in figure A.3.

We also had access to porosity data that was taken in one of the explorations carried out by the Geological Survey of Spain(IGME) [8]. In this exploration, some drill holes were drilled and porosity values were obtained from the extracted samples.

TABLE I: Laboratory porosity values.

	Porosity (%)	
Bh1'	13.607	A
BH2	9.9544	A
M1	11.232	C
M2	31.301	C
M3	14.945	C
M10	14.434	B

C. Procedures and discussion

In order to obtain the empirical laws describing the study area, the laws mentioned above have been adjusted with the porosity values in table I.
Initially, the original Archie equation and the seismic velocity equation without the clay content term were used. The values given to the constants were similar to those used by other authors for materials similar to the ones obtained. However, as very high porosities were obtained the fitting has been done using equations (2) and (3). An attempt to adjust the resistivity by considering the surface resistivity as seen in equation (5) was also made, but the adjustment was worse than without this term. For the velocity empirical laws, considering the content of clay improves results. Moreover, the description of the core samples [8] report the presence of clay. This apparent contradiction on the resistivity laws, is due to the fact that relation (5) from Rhoades is an unrefined relationship [9]. There are other relationships more refined but geochemical relationships are needed to use them.
Table II and table III show the constants and the different parameters adjusted for the empirical equations of resistivity and seismic velocity, respectively.

Table IV shows the mean porosities obtained. For cluster B and C, both values are quite similar and resemble the one obtained in the laboratory, being cluster B the best fit. However, in cluster A, the porosity estimated with the velocity model is higher than the one obtained in the laboratory.

TABLE II: Adjusted constants of the modified Archie equation for the different clusters.

Cluster	a	m	S_w	n
A	1.5	1.7	0.4	2.1
B1	0.7	1.4	0.4	2.2
B2	0.5	1.3	0.4	2.1
C1	1.4	1.7	0.3	1.8
C2	1.3	1.7	0.3	1

TABLE III: Adjusted constants of the empirical equation that relates p-wave seismic velocity to porosity.

Cluster	H_0	H_1	H_2	C
A	5	6.5	5	0.02
B1	4.5	5.4	2.18	0.3
B2	4.3	6.9	3.2	0.4
C1	4.6	9.3	5.87	0.3
C2	4.6	9.3	5.85	0.25

TABLE IV: Mean porosities obtained from seismic and resistivity tomographies models.

Cluster	Resistivity porosity(%)	Seismic porosity(%)
A	13.91	17.45
B1	14.79	14.15
B2	14.29	14.69
C1	20.05	23.13
C2	20.16	21.56

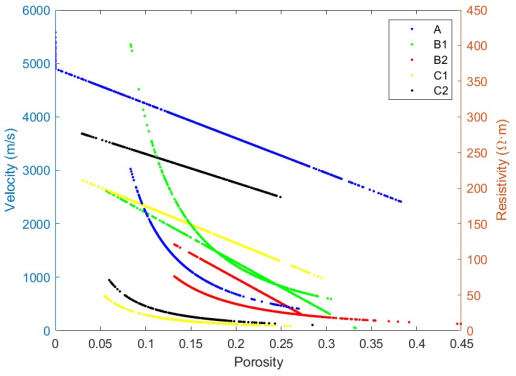

FIG. 6: Velocity and resistivity plot as function of the porosity.

In figure 6, straight line corresponds to seismic velocity as a function of porosity and curves corresponds to the resistivity.

Figure 8 shows the porosity variation in the profile for the model we have obtained with the empirical equations using seismic and resistivity models.There is a fairly good correspondence between the two figures although the porosity variations are sharper for the velocity model. Both images show how porosity decreases with depth due to mechanical compression. It can also be

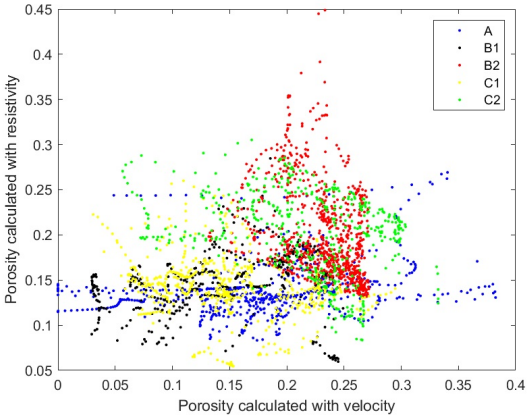

FIG. 7: Porosity calculated with the velocity model vs porosity calculated with the resistivity model.

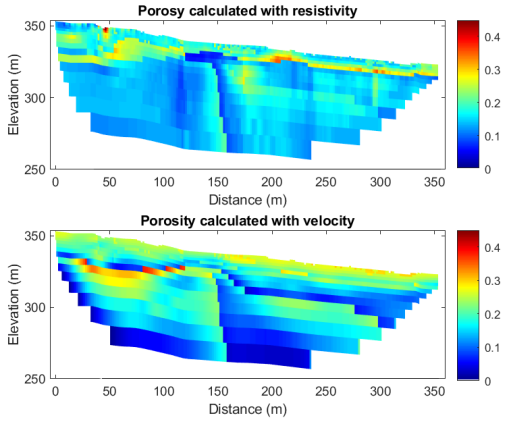

FIG. 8: Representation of porosity for the data obtained with both resistivity and seismic velocity models.

seen that where clusters A and B meet the porosity increases. This may be due to the fact that it is right where the fault is located. Therefore, there may be secondary porosity due to the fractured fault zone.

V. CONCLUSIONS

In this work we have found a first aproximation to the equations that relate porosity with p-wave propagation velocity and resistivity. The constants governing these equations have been found by trial and error, in the range of values used by other authors. However, when the geochemical components of the fluid are known, a better adjustment could be made by calculating the surface conductivity.

From the results obtained, it has been possible to distinguish the different components of the profile and how the porosity varies in them, decreasing with depth. It has also been possible to obtain a first approximation to the water saturation values, being greater in the the lower part of the profile.

Similar studies can be done in a bigger scale using result from magnetotelluric surveys. The information obtained about the porosity could be used as an input for a hydrological model for the study of fluid circulation in the reservoir. It could also be used to calculate the temperature distribution in the reservoir.

Acknowledgments

I would like to thank my advisor Pilar Queralt for all the time she has spent on helping me with this project and for encouraging me to continue in this branch of science. I would also like to thank my family and friends for loving and supporting me during these four years.

[1] Coskun, A., Bolatturk, A. Kanoglu, M. 1999. Thermodynamic and economic analysis and optimization of power cycles for a medium temperature geothermal resource. 2014. Energy Conversion and Management. 78, 39-49.

[2] Mitjanas, G., Ledo, J., Macau, A, Alías, G., Queralt, P., Bellmunt, F., Rivero, Ll., Gabàs, A., Marcuello, A., Benjumea, B., Martí, A., Figueras, S. 2021. Integrated seismic ambient noise, magnetotellurics and gravity data for the 2D interpretation of the Vallès basin structure in the geothermal system of La Garriga-Samalús (NE Spain). Geothermics. 93, 102067.

[3] Roca, E., Sans, M., Cabrera, L. Marzo, M. 1999. Oligocene to Middle Miocene evolution of the central Catalan margin (northwestern Mediterranean). Tectonophysics 315, 209–229.

[4] García-Yeguas, A., Ledo, J., Piña-Varas, P., Prudencio, J., Queralt, P., Marcuello, A., Ibañez, J., Benjume, B., Sánchez-Alzola, A., Pérez, N. 2017. A 3D joint interpretation of magnetotelluric and seismic tomographic models: The case of the volcanic island of Tenerife. Computer and Geosciences. 109, 95-105.

[5] Mitjanas, G. 2018. Multiscale characterization of fracture zones and the role of fluids: Geophysical and petrological study of the Vallès fault in Samalús (NE Spain). Master thesis.

[6] Kirsch, Reinhard. Groundwater Geophysics, 2nd. ed. Postdam: Springer, 2006, 1-22. 978-3-540-88404-0.

[7] Mitjanas, G. 2021. Personal comunication.

[8] IGME, 1984. Proyecto de investigación geotérmica en el Vallés mediante sondeos de reconocimiento y síntesis hidrogeotérmica. Control geotermico de los sondeos SAMALUS 2, 3, 4 y 5.

[9] Bosch, D. 2015. Tomografia elèctrica a escala de laboratori: investigació del sistema roca-salmorra-CO_2. PhD thesis.

Appendix A

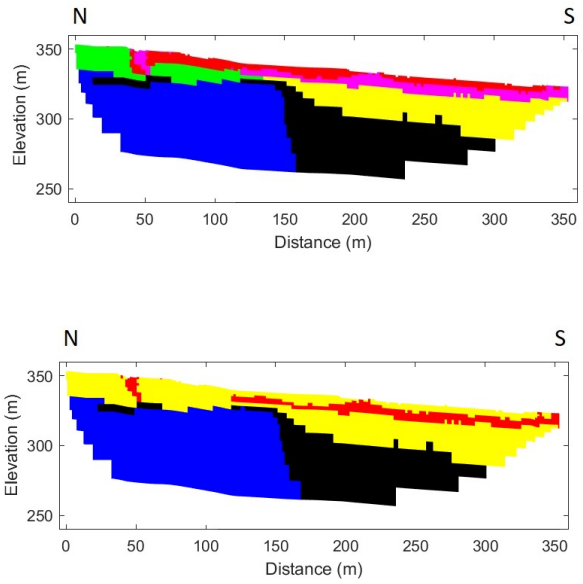

FIG. A.1: Representation of the different clusters when tried for n=6 and 4 respectively.

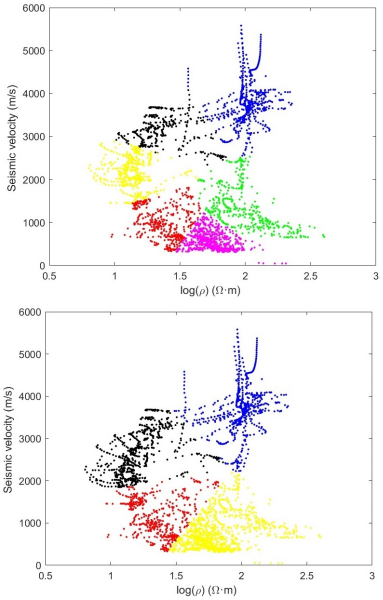

FIG. A.2: Plot of seismic velocity versus resistivity for the different clusters with n=6 and 4 respectively.

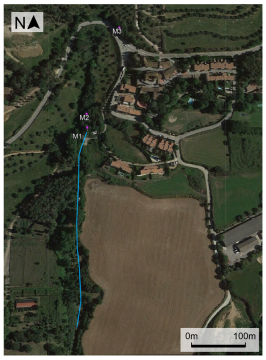

FIG. A.3: Position where the samples to calculate porosity were taken.